

Case Report

## Spontaneous cutaneous soft tissue sarcoma with differentiation into fibroblasts in a Sprague-Dawley rat

Takashi Ogawa<sup>1\*</sup>, Tomoya Onozato<sup>1</sup>, Yuji Okuhara<sup>1</sup>, Tatsuya Nagasawa<sup>1</sup>, Toru Tamura<sup>1</sup>, and Morimichi Hayashi<sup>1</sup>

<sup>1</sup>Toxicology Research Laboratory, R&D, Kissei Pharmaceutical Co., Ltd., 2320-1 Maki, Hotaka, Azumino, Nagano 399-8305, Japan

**Abstract:** A small mass with an ulcer was found in the skin of the dorsal cervix of a 7-month-old male Sprague-Dawley rat. Histologically, the central region of the tumor showed a high cellular density with oval-shaped tumor cells arranged in an alveolar pattern and thin collagen fiber bundles. The peripheral region of the tumor had a low cellular density with short spindle- or polygonal-shaped tumor cells surrounded by abundant collagen fiber bundles. Immunohistochemically, the tumor cells were strongly positive for vimentin and proliferating cell nuclear antigen, and a portion of the short spindle- or polygonal-shaped cells located in the peripheral region of the tumor were positive for S100A4. However, the tumor cells were negative for alpha-smooth muscle actin, desmin, S100, chromogranin A, neurofilament, CD68, Iba-1, cytokeratin 20, von Willebrand factor, melanosome, and anti-melanoma. Electron microscopically, the tumor cells had an abundance of rough endoplasmic reticulum, the Golgi apparatus, and a few intracellular collagen fibrils, showing fibroblastic features. Considering the lack of diagnostic differentiation, the tumor was diagnosed as an undifferentiated malignant mesenchymal tumor and classified as a soft tissue sarcoma with differentiation into fibroblasts in a portion of the tumor cells. (DOI: 10.1293/tox.2015-0069; *J Toxicol Pathol* 2016; 29: 119–124)

**Key words:** soft tissue sarcoma, Sprague-Dawley rat, fibroblast, collagen fiber

There are many reports on the incidence of spontaneous tumors in Sprague-Dawley (SD) rats; however, the incidence of individual tumors differs depending on the report. Of these spontaneous tumors in SD rats, the incidence of cutaneous or subcutaneous soft tissue tumors is relatively high: 13% in males and 6.9% in females in one report<sup>1</sup>. Fibroma is the most frequent cutaneous or subcutaneous soft tissue tumors, with fibrosarcoma, lipoma, schwannoma, rhabdomyosarcoma, and hemangioma also occurring at a low frequency<sup>2–4</sup>. Although soft tissue tumors are derived from various origins, they occasionally show similar histological features, and thus it is sometimes difficult to diagnose soft tissue tumors by histological findings alone. In such cases, immunohistochemical and ultrastructural findings have a key role in their diagnosis, but even so, there are few cases in which the cell origin is not defined. Here we report the histological, immunohistochemical, and ultrastructural features of a case of spontaneous cutaneous soft tissue sarcoma having no definite cell origin in the cervical

region of a male SD rat.

A 7-month-old male Crl:CD (SD) rat was purchased from Charles River Laboratories Japan, Inc (Yokohama, Japan). A small mass with an ulcer was found in the skin of the dorsal cervix of the animal on its arrival. The animal was used in a 4-week repeated oral administration study to evaluate the pharmacological response of a compound, which was under development as a pharmaceutical agent, and was necropsied at 8 months of age after completion of the study. The mass showed no change in appearance throughout the study. At necropsy, the mass was approximately 8 × 7 × 6 mm in size, and the cut surface was milky white in color with poor demarcation from the surrounding tissue. No other gross lesions were observed in any organs. The animal experiment complied with the Guide for Care and Use of Experimental Animals of the Toxicology Research Laboratory, Kissei Pharmaceutical Co., Ltd.

The mass was fixed in 10% phosphate-buffered formalin, embedded in paraffin, cut into 3 μm sections, and stained with hematoxylin-eosin (HE) for microscopic examination. Additional histochemical stains, including Masson's trichrome, Watanabe's silver impregnation, alcian blue (AB), periodic acid-Schiff (PAS), and toluidine blue, were also used. Immunohistochemical staining was carried out with an EnVision™ + Dual Link System-HRP kit (Dako A/S, Glostrup, Denmark) and antibodies to vimentin, pancytokeratin, S100A4, alpha-smooth muscle actin (SMA), desmin, S100, chromogranin A, neurofilament, CD68, Iba-

Received: 14 October 2015, Accepted: 23 January 2016

Published online in J-STAGE: 25 February 2016

\*Corresponding author: T Ogawa

(e-mail: takashi\_ogawa@pharm.kissei.co.jp)

©2016 The Japanese Society of Toxicologic Pathology

This is an open-access article distributed under the terms of the Creative Commons Attribution Non-Commercial No Derivatives (by-nc-nd) License <<http://creativecommons.org/licenses/by-nc-nd/4.0/>>.

**Table 1.** Antibodies Used for Immunohistochemistry

Antibody	Manufacturer (city, state, country)	Host species	Clonality (clone name)
CD68	Thermo Fisher Scientific, Inc. (Waltham, MA, USA)	Mouse	Monoclonal (KP1)
Chromogranin A	Dako (Glostrup, Denmark)	Rabbit	Polyclonal
Cytokeratin	Dako	Mouse	Monoclonal (AE1/AE3)
Cytokeratin 20	Dako	Mouse	Monoclonal (K <sub>s</sub> 20.8)
Desmin	Thermo Fisher Scientific, Inc.	Rabbit	Polyclonal
Iba-1 (AIF-1)	Bioss Inc. (Woburn, MA, USA)	Rabbit	Polyclonal
Melanosome	GeneTex, Inc. (Irvine, CA, USA)	Mouse	Monoclonal (HMB45)
Melanoma	Dako	Mouse	Monoclonal (PNL2)
Neurofilament	Dako	Mouse	Monoclonal (2F11)
Proliferating cell nuclear antigen	Dako	Mouse	Monoclonal (PC10)
S100	Dako	Rabbit	Polyclonal
S100A4	Thermo Fisher Scientific, Inc.	Rabbit	Polyclonal
Vimentin	Dako	Mouse	Monoclonal (V9)
Von Willebrand Factor	AbD Serotec (Kidlington, Oxford, UK)	Mouse	Monoclonal (21-43)
Alpha smooth muscle actin	Dako	Mouse	Monoclonal (1A4)

1, cytokeratin 20, von Willebrand factor, melanosome, anti-melanoma, and proliferating cell nuclear antigen (PCNA). The sources and clones of these antibodies are shown in Table 1. The terminal deoxyribonucleotide transferase-mediated dUTP nick end labeling (TUNEL) method was used to examine the presence of apoptotic cells using a TACS2 TdT In Situ Apoptosis Detection Kit (Trevigen, MD, USA). For electron microscopic examination, pieces of the formalin-fixed tissue were immersed in a half-strength Karnovsky solution and fixed in 1% osmium tetroxide. Ultrathin sections were stained with uranyl acetate and lead citrate, evaporated with carbon, and observed under a transmission electron microscope (JEM-1200EX, JEOL Ltd., Tokyo, Japan).

Histologically, the tumor showed a solid growth pattern and was located in the dermis without continuity with the epidermis (Fig. 1a). It was nonencapsulated and poorly demarcated from the surrounding tissue. The epidermis covering the tumor was mostly ulcerated and partially acanthotic. Lymphocytes were diffusely infiltrated into the tumor, in addition to neutrophil infiltration around the ulcer. Many capillary vessels with congestion were found in the tumor, particularly just below the ulcer. Tumor cells with scant amphophilic cytoplasm and oval-shaped nuclei including one or two nucleoli invaded into adjacent connective tissue in the dermis, involving hair follicles and sebaceous glands with normal structures (Fig. 1b). In the central region of the tumor, which had a high cellular density, the tumor cells were oval shaped and arranged in an alveolar pattern with thin bundles of fibrous tissue (Fig. 1c and 1d). In the peripheral region of the tumor with a low cellular density, the tumor cells were short spindle or polygonal shaped and surrounded by more abundant bundles of fibrous tissue (Fig. 1e and 1f). Mitotic figures were frequent in the central region (Fig. 1d). Masson's trichrome staining and Watanabe's silver impregnation revealed that the fibrous tissue consisted of mostly collagen fibers and partially reticular fibers (Fig. 2a). AB-positive myxoid matrix was present in the peripheral region of the tumor. Some of the tumor cells had PAS-positive fine granules digested by amylase.

No metachromasia was observed with toluidine blue.

Immunohistochemical analyses revealed that the tumor cells were strongly positive for vimentin and negative for cytokeratin (Fig. 2b). A portion of the short spindle- or polygonal-shaped cells located in the peripheral region of the tumor were positive for S100A4, also called fibroblast-specific protein-1 (Fig. 2c). On the other hand, all of the tumor cells were negative for markers of epithelial cells (cytokeratin 20), muscle cells (SMA, desmin), histiocytes (CD68, Iba-1), melanocytes (melanosome, melanoma), nerve fibers (S100, neurofilament), neuroendocrine cells (chromogranin A), and vascular endothelial cells (von Willebrand factor). PCNA-positive cells were more abundant in the central region than in the peripheral region of the tumor (Fig. 2d). In contrast, TUNEL-positive cells were found with higher frequency in the peripheral region than in the central region of the tumor. Most of the PCNA-positive cells had an oval nucleus.

Electron microscopically, the tumor cells surrounded by collagen fibrils had an abundance of rough endoplasmic reticulum and the Golgi apparatus (Fig. 3a and 3b). In the peripheral region of the tumor, some of the tumor cells had cell processes surrounding collagen fibrils and a few intracellular collagen fibrils (Fig. 3c and 3d). No melanosomes, premelanosomes, basal lamina, or cell junctions were identified, but few lysosomes were identified.

In this case, a small mass with an ulcer was found in the dermis of a male SD rat. The mass consisted of proliferating cells with a variety of shapes such as oval, short spindle or polygonal, showing a solid growth pattern with collagen fibers. Immunohistochemical analyses revealed that the proliferating cells were strongly positive for vimentin and negative for cytokeratin, indicating that they derived from mesenchymal cells. A portion of the proliferating cells exhibited fibroblastic ultrastructural features.

The differential diagnosis between an exaggerated fibroblastic response to tissue injury and a mesenchymal tumor is usually made on the basis of size and growth pattern<sup>5</sup>. PCNA immunoreactivity is also useful in differentiating in-

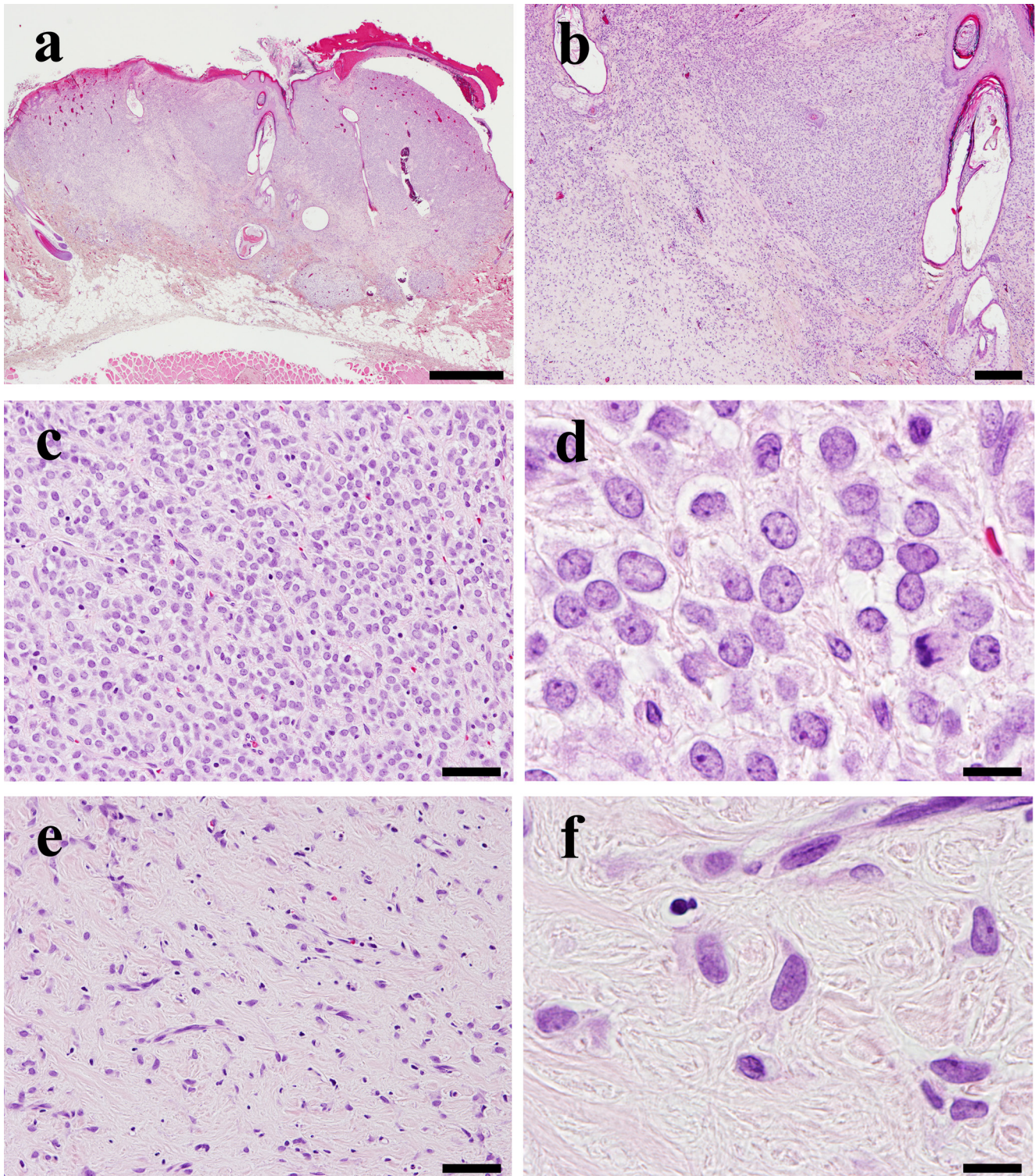


**Fig. 1.** Histological appearance of the tumor. Hematoxylin-eosin staining. a) The small mass with an ulcer showed a solid growth pattern and was located in the dermis. b) The tumor cells were invasive to adjacent connective tissue in the dermis, involving hair follicles and sebaceous glands with normal structures. c) In the central region of the tumor, which had a high cellular density, the tumor cells were arranged in an alveolar pattern with thin bundles of fibrous tissue. d) Higher magnification of Fig. 1c. The tumor cells were oval shaped with scant amphophilic cytoplasm and oval-shaped nuclei including one or two nucleoli. Mitotic figures were frequent. e) In the peripheral region of the tumor, which had a low cellular density, the tumor cells were surrounded by abundant bundles of fibrous tissue. f) Higher magnification of Fig. 1e. The tumor cells were short spindle or polygonal shaped. Bars = 1 mm (a), 200  $\mu$ m (b), 50  $\mu$ m (c, d), 10  $\mu$ m (e, f).

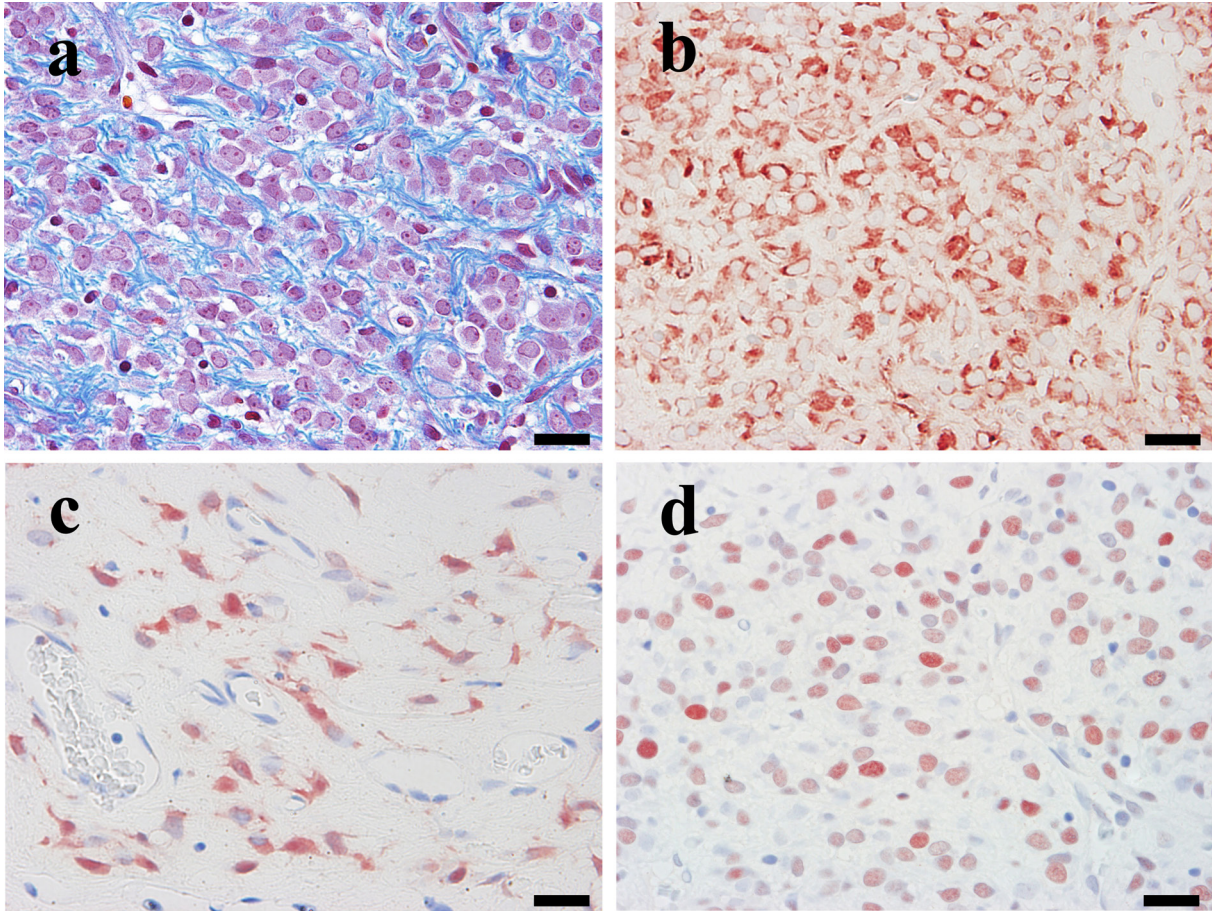


**Fig. 2.** Histochemical staining and immunostaining of the tumor. a) Masson's trichrome staining. The collagen fibers surrounding the tumor cells were stained blue. b) Vimentin immunostaining. The tumor cells were strongly positive for vimentin. c) S100A4 immunostaining. A portion of the short spindle- or polygonal-shaped cells located in the peripheral region of the tumor were positive for S100A4. d) PCNA immunostaining. The tumor cells were positive for PCNA. Bars = 20  $\mu$ m.

cipliant sarcoma<sup>6</sup>. In this case, the lesion was small and composed of polymorphic cells invading surrounding tissues with no destruction of the skin appendages. Therefore, it was difficult to determine whether the lesion was neoplastic or nonneoplastic by HE staining alone. However, also considering the results of immunohistochemical staining, it was judged that the lesion was neoplastic and consisted of undifferentiated malignant mesenchymal cells due to positive reactions for PCNA and vimentin and negative reactions for all other differentiation markers. Moreover, the presence of abundant collagen fibers required a differential diagnosis of mesenchymal tumors producing collagen fibers, such as fibrosarcoma, malignant fibrous histiocytoma, melanoma, leiomyosarcoma, and malignant peripheral nerve sheath tumor. However, no immunoreactivity for the markers of histiocytes, melanocytes, muscle cells, or nerve fibers was detected in the tumor, and therefore fibrosarcoma was considered to be the most significant differential diagnosis.

Regarding fibrosarcoma, there are no validated diagnostic or prognostic markers, and immunohistochemistry shows absent expression of any markers other than vimentin

or very limited expression of SMA<sup>7, 8</sup>. S100A4, fibroblast-specific protein-1, for which some of the tumor cells in the present study were positive, is also not a highly specific marker for fibroblasts, since it has been reported to be expressed in metastatic tumors and in normal cells, including fibroblasts, macrophages, lymphocytes, and bone marrow-derived cells<sup>9</sup>. The important features in diagnosis of a tumor as fibrosarcoma are that it is of mesenchymal origin and that the spindle cells making up a large part of it are arranged in a 'herring-bone' pattern with abundant collagen fibers. Electron microscopically, fibrosarcoma cells contain an abundance of rough endoplasmic reticulum and the Golgi apparatus and sometimes contain intracellular collagen fibrils, which is a phenomenon associated with the rapid synthesis of collagen<sup>10, 11</sup>. In this case, the immunohistochemical and ultrastructural features were consistent with those of fibrosarcoma, and at least a portion of the tumor cells distinctly showed differentiation into fibroblasts with intracellular collagen fibrils. However, oval cells were arranged in an alveolar pattern in the central region of the tumor, accounting for approximately half of the tumor, and

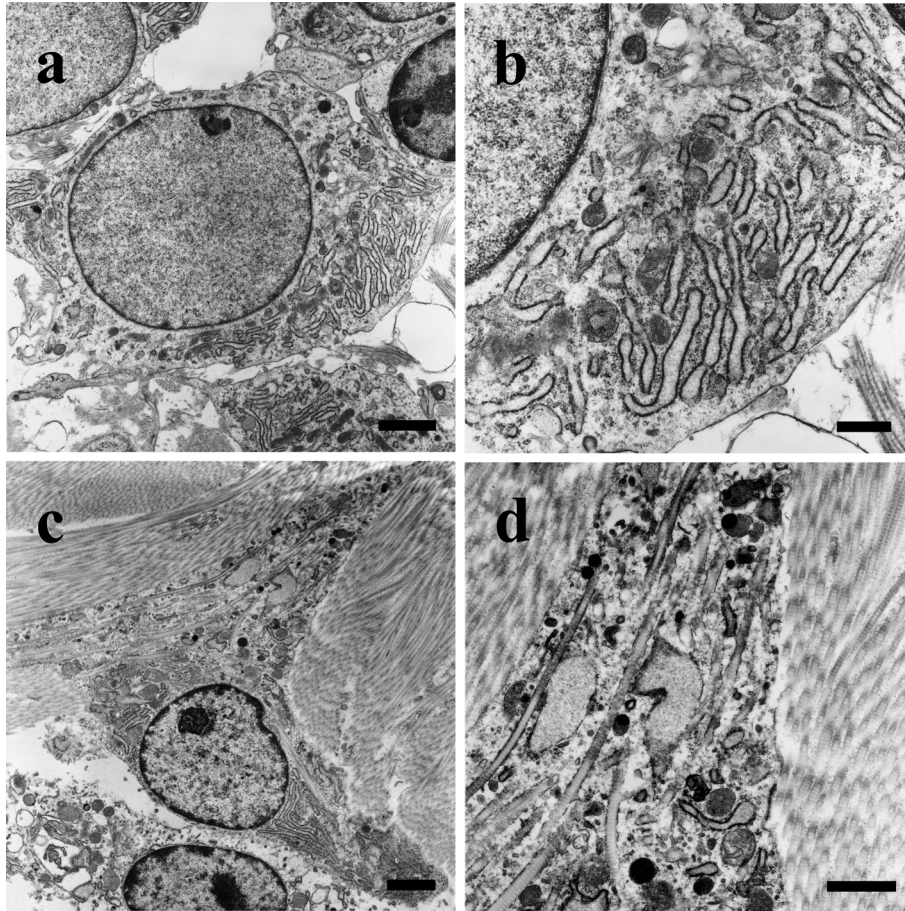


**Fig. 3.** Ultrastructural appearance of the tumor cells. a) The tumor cells had an abundance of rough endoplasmic reticulum. b) High magnification of Fig. 3a. c) The tumor cells in the peripheral region of the tumor had a few intracellular collagen fibrils. d) High magnification of Fig. 3c. Bars = 2  $\mu\text{m}$  (a, c), 500 nm (b), 1  $\mu\text{m}$  (d).

spindle cells located in the peripheral region of the tumor also showed no typical herring-bone pattern. Considering these features, sufficient evidence to diagnose fibrosarcoma seems to be lacking in this case. Taken together, this case with no definite evidence of cell origin was diagnosed as a soft tissue sarcoma with differentiation into fibroblasts in a portion of the tumor cells.

**Acknowledgments:** We are grateful to Yoshimi Tukahara, Rie Nakano, and Sayuri Yamagishi for their excellent technical assistance. We would also like to express our appreciation to Dr. Masahiro Tsutsumi, Department of Pathology, Saiseikai-Chuwa Hospital, Japan, Dr. Gary A Boorman, Nonclinical Safety Assessment, Covance Laboratories Inc., USA, and Dr. Susan A. Elmore, National Toxicology Program, National Institute of Environmental Health Sciences, USA, for their review and helpful comments.

**Disclosure of Potential Conflicts of Interest:** The authors declare that they have no conflicts of interest.

## References

1. Muraoka Y, Itoh M, Yamashita F, and Hayashi Y. [Spontaneous tumors in aged SD-JCL rats (author's transl)]. *Jikken Dobutsu*. **26**: 13–22. 1977. [[Medline](#)]
2. Imai K, and Yoshimura S. Spontaneous tumors in Sprague-Dawley (CD:Crj) rats. *J Toxicol Pathol*. **1**: 7–12. 1988. [[CrossRef](#)]
3. Morii S, and Fujii T. [Spontaneous tumors in Sprague-Dawley JCL rats (author's transl)]. *Jikken Dobutsu*. **22**: 127–138. 1973. [[Medline](#)]
4. Kaspereit J, and Rittinghausen S. Spontaneous neoplastic lesions in Harlan Sprague-Dawley rats. *Exp Toxicol Pathol*. **51**: 105–107. 1999. [[Medline](#)] [[CrossRef](#)]
5. Greaves P, Chouinard L, Ernst H, Mecklenburg L, Prui-boom-Brees IM, Rinke M, Rittinghausen S, Thibault S, Von Erichsen J, and Yoshida T. Proliferative and non-proliferative lesions of the rat and mouse soft tissue, skeletal muscle and mesothelium. *J Toxicol Pathol*. **26**(Suppl): 1S–26S. 2013. [[Medline](#)] [[CrossRef](#)]
6. Kirkpatrick CJ, Alves A, Köhler H, Kriegsmann J, Bitteringer F, Otto M, Williams DF, and Eloy R. Biomaterial-induced sarcoma: A novel model to study preneoplastic change. *Am J Pathol*. **156**: 1455–1467. 2000. [[Medline](#)] [[CrossRef](#)]

7. Banerji N, and Kanjilal S. Comparative genomic profiling of fibrosarcoma using a feline model. *Cancer Res.* **67**(9 Suppl): 2972. 2007.
8. Folpe AL. Fibrosarcoma: a review and update. *Histopathology.* **64**: 12–25. 2014. [[Medline](#)] [[CrossRef](#)]
9. Li ZH, Dulyaninova NG, House RP, Almo SC, and Bresnick AR. S100A4 regulates macrophage chemotaxis. *Mol Biol Cell.* **21**: 2598–2610. 2010. [[Medline](#)] [[CrossRef](#)]
10. Eyden B. Fibroblast phenotype plasticity: relevance for understanding heterogeneity in “fibroblastic” tumors. *Ultrastruct Pathol.* **28**: 307–319. 2004. [[Medline](#)] [[CrossRef](#)]
11. Ghadially FN. *Ultrastructural pathology of the cell and matrix*, 3rd ed. Butterworths, London. 1988.